Volume 139 | Number 16 | 21 August 2014 | Pages 3813–4090

# Analyst

www.rsc.org/analyst

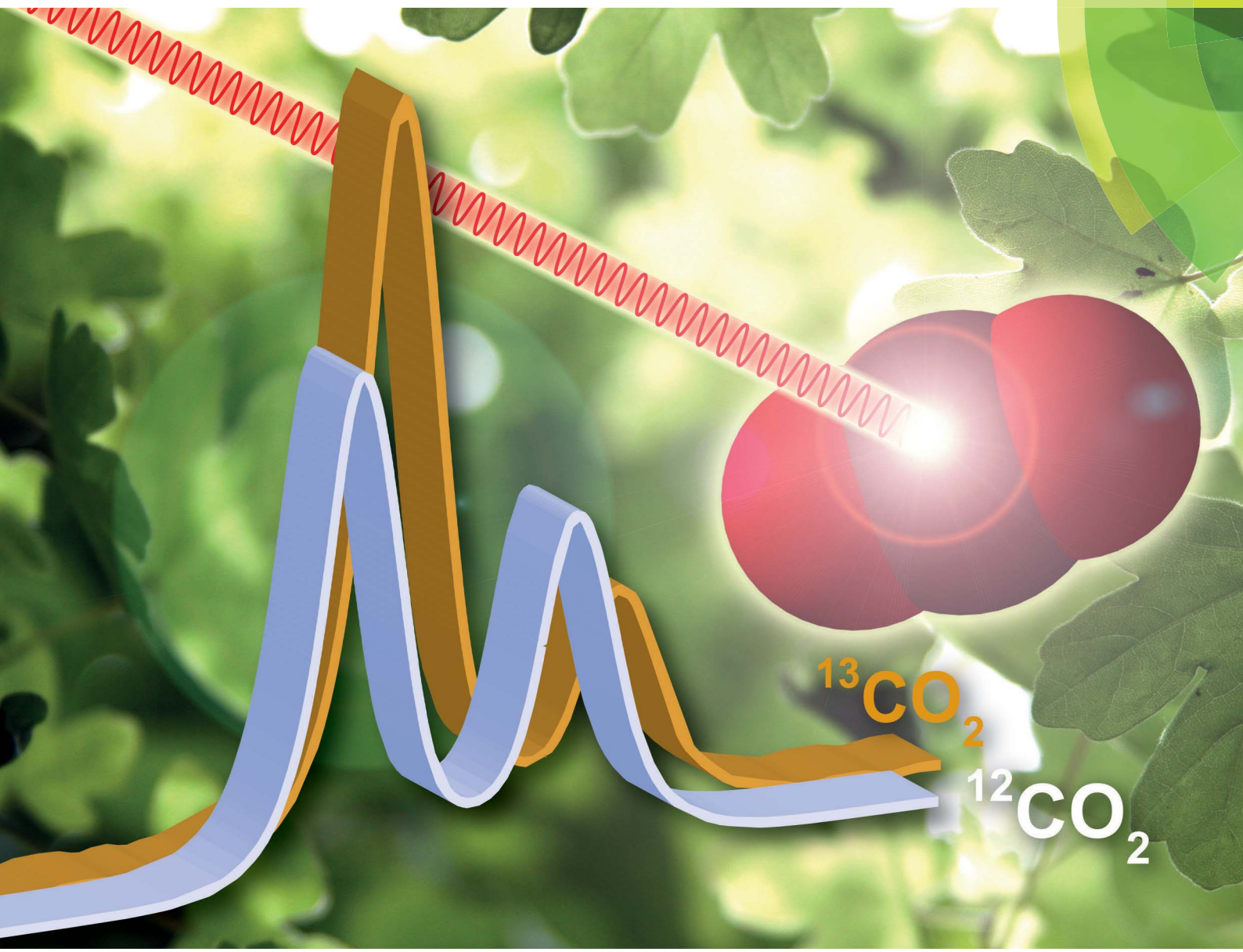


ISSN 0003-2654

ROYAL SOCIETY OF CHEMISTRY

PAPER

Torsten Frosch *et al.*

Enhanced Raman multigas sensing – a novel tool for control and analysis of $^{13}CO_2$ labeling experiments in environmental research

Analyst

PAPER

View Article Online
View Journal | View Issue



Cite this: *Analyst*, 2014, **139**, 3879

# Enhanced Raman multigas sensing – a novel tool for control and analysis of $^{13}CO_2$ labeling experiments in environmental research

Robert Keiner,[ab] Torsten Frosch,*[ab] Tara Massad,[c] Susan Trumbore[c] and Jürgen Popp[abd]

Received 19th October 2013
Accepted 4th March 2014

DOI: 10.1039/c3an01971c

www.rsc.org/analyst

Cavity-enhanced Raman multigas spectrometry is introduced as a versatile technique for monitoring of $^{13}CO_2$ isotope labeling experiments, while simultaneously quantifying the fluxes of $O_2$ and other relevant gases across a wide range of concentrations. The multigas analysis was performed in a closed cycle; no gas was consumed, and the gas composition was not altered by the measurement. Isotope labeling of plant metabolites *via* photosynthetic uptake of $^{13}CO_2$ enables the investigation of resource flows in plants and is now an important tool in ecophysiological studies. In this experiment the $^{13}C$ labeling of monoclonal cuttings of *Populus trichocarpa* was undertaken. The high time resolution of the online multigas analysis allowed precise control of the pulse labeling and was exploited to calculate the kinetics of photosynthetic $^{13}CO_2$ uptake and to extrapolate the exact value of the $^{13}CO_2$ peak concentration in the labeling chamber. Further, the leaf dark respiration of immature and mature leaves was analyzed. The quantification of the photosynthetic $O_2$ production rate as a byproduct of the $^{13}CO_2$ uptake correlated with the amount of available light and the leaf area of the plants in the labeling chamber. The ability to acquire $CO_2$ and $O_2$ respiration rates simultaneously also simplifies the determination of respiratory quotients (rate of $O_2$ uptake compared to $CO_2$ release) and thus indicates the type of combusted substrate. By combining quantification of respiration quotients with the tracing of $^{13}C$ in plants, cavity enhanced Raman spectroscopy adds a valuable new tool for studies of metabolism at the organismal to ecosystem scale.

## Introduction

Isotope labeling with gaseous precursors is an important tool in ecophysiological studies as it allows for a detailed investigation of the flow of resources at the level of an individual organism up to an entire ecosystem. For example, by labeling with $^{13}C$, the existence of different carbon allocation patterns between plant functional groups[1] and the fast transfer of recently assimilated carbon to soil microorganisms[2] have been demonstrated. $^{13}C$ labeling has also been used at a molecular level to understand plant investments in secondary metabolites that serve as antiherbivore defenses[3] as well as the biosynthetic pathways leading to defense-related compounds.[4] Chemical ecology studies have monitored photosynthetic uptake of $^{13}CO_2$ in real time in order to measure the incorporation of newly assimilated $^{13}C$ into primary *versus* secondary metabolites under simulated herbivore pressure[4,5] to address the growth-defense hypothesis.[6] Measuring gas exchange of both $^{13}CO_2$ and $^{12}CO_2$ is important for investigations of the balance of the amount of incorporated $^{13}C$ *versus* the amount of respirationally released $^{13}CO_2$. $^{13}C$ labeling of plants *via* exposure to pulses of $^{13}CO_2$ is becoming a more commonly employed tool in studies of plant physiology and chemical ecology.[7]

Nowadays, in most plant respiration experiments, $CO_2$ production is measured as the sole parameter, either electrochemically or by non-dispersive infrared absorption spectroscopy.[8] However, $O_2$ consumption is also important for the determination of the respiratory quotient in order to draw conclusions about the type of combusted substrate and for quantification of the amount of label that got fixed by the plant. Most commonly used methods are not sufficiently sensitive in the measurement of $O_2$ in plant respiration over timescales of minutes. High sensitivity $O_2$ measurements are currently performed by taking gas samples for successive lab-based analyses using gas chromatography (GC) in combination with mass spectrometry (GCMS) in order to determine $O_2/N_2$ ratios. Unfortunately, these chromatographic techniques are slow, consumptive, and expensive, because the samples consist of complex mixtures of gases at various concentrations and several expensive test gases are needed for instrument calibration. To date, the miniaturization of test equipment for rapid online monitoring of multigas-samples (consisting of $O_2$, $N_2$, $^{13}CO_2$ and $^{12}CO_2$) has been limited.

[a]*Institute of Photonic Technology, Jena, Germany. E-mail: torsten.frosch@uni-jena.de*
[b]*Friedrich-Schiller University, Institute for Physical Chemistry, Jena, Germany*
[c]*Max-Plack-Institute for Biogeochemistry, Jena, Germany*
[d]*Friedrich-Schiller University, Abbe School of Photonics, Jena, Germany*

These limitations can be circumvented by Raman spectroscopy, which provides characteristic information about molecular vibrations[9] and thus chemical specificity. Raman spectroscopy emerged in recent years as an extremely powerful method[10] in various natural science disciplines[11] to investigate solid samples, liquids, and gases. Raman gas analysis is capable of quantifying almost all gases (except noble gases) simultaneously with just one measurement.[12] This work introduces the methodology of cavity enhanced Raman multigas spectroscopy for pulse labeling studies of plant physiology.

## Experimental details

Monoclonal cuttings of *Populus trichocarpa* were obtained from the "Thüringer Landesanstalt für Landwirtschaft", Dornburg (Germany). *Populus trichocarpa* is a fast-growing species native to western North America. Cuttings were individually planted in 2 l pots with potting soil (Klasmann KKS Bio Topfsubstrat 27) mixed 1 : 1 with quartz sand and grown in the greenhouse with additional light (Son-T Agro 430 W HPS bulbs, primary light range 520–610 nm, Philips Lighting Company, New Jersey, USA) from 6:00–17:00. The pots were uniformly watered with an irrigation system that delivered water two to three times for 3 min between 12:00 and 13:00 each day, depending on the temperature. The plants were moved to a climate chamber and exposed to five days of gradual cooling followed by an artificial winter of 8 h 10 °C days and 4 °C nights to induce senescence and leaf fall. The plants were returned to the greenhouse and exposed to the previous light and water conditions. As leaves were flushing, plants were exposed to $^{13}CO_2$ in a 2 $m^3$ labeling chamber (see Fig. 2). The gas phase was homogenized with the help of fans. Twenty-three to 25 plants were labeled on two consecutive days (runs 1 and 2, see Table 1) for approximately 2 h from 12:00 to 14:00. $^{13}CO_2$ was introduced into the chamber *via* acidification of 2.67 g followed by 1.33 g 99% $NaH^{13}CO_3$ (Cambridge Isotope Laboratories, USA) with 16 ml or 8 ml diluted hydrochloric acid. The leaf area of every plant was measured at the time of labeling.

## Results and discussion

### Raman gas monitoring of multigas mixtures containing isotopic labeled gases

The Raman gas sensor consists of a miniaturized laser diode with $\lambda_{exc.} = 650$ nm and a cw output power of 50 mW. This diode is passively frequency locked and feedback-coupled to a high-finesse cavity (PCB) enabling a power build-up to 100 W. Thus a strong signal enhancement is achieved with only low power consumption of the instrument. The PCB supports a Gaussian beam and consists of an input coupler mirror and an end mirror, both with extremely low scattering losses and transmission. For optimal beam enhancement and stable operation, the cavity components are aligned for spatial mode matching of the input beam and the Gaussian beam supported by the PBC while the facet of the laser diode helps in stabilizing mode matching by spatial filtering.[13] This arrangement of the PCB is extremely stable to mechanical vibrations and is connected to a high-throughput spectrometer with a room temperature operated charge coupled device (CCD) with 512 pixels and a spectral resolution of approx. 50 $cm^{-1}$. Additional sensors monitor the laser intensity, pressure and temperature for reliable gas quantification. With the help of this strong signal enhancement it was possible to monitor concentration fluctuations of about 50 to 100 ppm within measurement times of one second. The device was calibrated for the relevant gases, $N_2$, $O_2$, $^{12}CO_2$, and $^{13}CO_2$, by flushing the optical cavity with pure gases. Underground correction was accomplished by subtracting the spectrum of the Raman inactive noble gas argon. $^{13}CO_2$ was calibrated with a GCMS-validated 1% mixture of $^{13}CO_2$ with 99% argon (Raman inactive noble gas). The calibrated reference spectra are a prerequisite for the online quantification of sample gases during the isotope labeling experiment (Fig. 1). A straightforward calibration approach is feasible because the Raman intensity, $I_{Stokes}$, scales strictly linearly with the gas density in molecules per volume, $nV^{-1}$, laser power, $I_0$, and partial pressure, $p$ over the whole dynamic range.

$$I_{Stokes} \sim \frac{n}{V} I_0 p \tag{1}$$

Next, a least square fit of the measured spectrum and the calibrated reference spectra provided the concentrations of the individual gases. Therefore an over-determined linear equation system was solved with the calibration gas, g, measured gas, a (mixture of gases), intensity, $I(\tilde{\nu})$, concentration, $c$, CCD pixel, $n$, and number, $m$, of extracted gases.

$$\begin{bmatrix} I(\tilde{\nu})_{g_1 1} & \cdots & I(\tilde{\nu})_{g_m 1} \\ \vdots & \ddots & \vdots \\ I(\tilde{\nu})_{g_1 n} & \cdots & I(\tilde{\nu})_{g_m n} \end{bmatrix} \begin{bmatrix} c_1 \\ \vdots \\ c_m \end{bmatrix} = \begin{bmatrix} I(\tilde{\nu})_{a1} \\ \vdots \\ I(\tilde{\nu})_{an} \end{bmatrix} \tag{2}$$

Another major advantage of Raman multigas sensing becomes obvious from eqn (2), namely that all gases which

Table 1 Comparison of the Raman gas monitoring of two labeling runs with different leaf areas and available photosynthetically active radiation (PAR) in the labeling chamber. The amount of developed oxygen, mean PAR, total leaf area and the exponential decay time $t_e$ are given. The oxygen production rate is higher and the $CO_2$ uptake is faster with higher light intensity and larger leaf area in labeling run 2. $t_e$ represents the decay time until the concentration decreased to 1/$e$ of its initial value based on the exponential fit equation: $c = c_0 e^{-t_e^{-1} t}$

| Labeling run | $O_2$ production [mol $d^{-1}$] | Light intensity PAR [W $m^{-2}$] | Total leaf area [$m^2$] | $^{13}CO_2$-uptake 1st dose $t_e$ [min] | $^{13}CO_2$-uptake 2nd dose $t_e$ [min] |
|---|---|---|---|---|---|
| 1 | 0.35 | 121 | 2.29 | 23.52 | 20.6 |
| 2 | 0.38 | 275 | 3.11 | 17.16 | 15.7 |

 

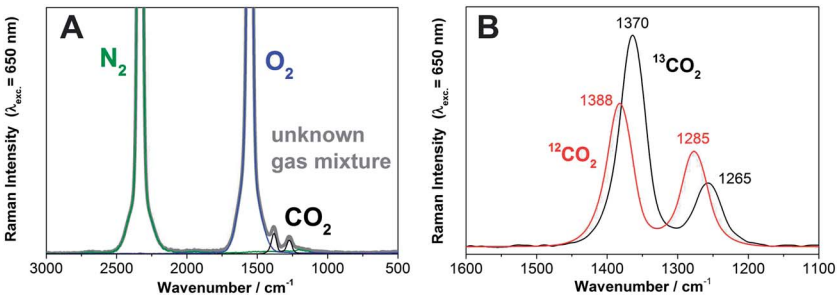


Fig. 1 (A) Example of a Raman gas spectrum ($\lambda_{exc.}$ = 650 nm) during a typical leaf dark respiration measurement of *Populus trichocarpa*. The Raman spectrum of the unknown gas mixture (grey) and the Raman spectra of the individual gaseous components (green: $N_2$, blue $O_2$, black $CO_2$) are shown ($N_2$ and $O_2$ are ro–vibrational spectra, with unresolved O and S branches). The concentrations of the individual gases can be deconvoluted from the experimentally acquired envelope. (B) The Raman gas spectra of $^{12}CO_2$ and $^{13}CO_2$ can be distinguished and simultaneously quantified due to their spectral shift and differences in the intensity distribution of the Fermi diad.

appear in course of a labeling experiment will be detected in the Raman spectrum of the multigas-mixture. Thus, if the difference between the experimental multigas-spectrum and the deconvoluted individual spectra differs from a zero-baseline, more information about additional gases can be obtained by data post-processing with an increased number, *m*, of extracted gases. An example spectrum of an experimental gas mixture and the spectra of the gaseous components ($N_2$, $O_2$, and $CO_2$) are depicted in Fig. 1A. The Raman gas spectra of the chemically similar gaseous isotopes, $^{12}CO_2$ and $^{13}CO_2$, can be readily distinguished due to their spectral shift and differences in the intensity pattern of the Fermi diad[14] (Fig. 1B). Thus, all relevant gases ($N_2$, $O_2$, $^{12}CO_2$, and $^{13}CO_2$) can be quantified individually and simultaneously with no cross-sensitivity. The gas concentrations ($N_2$, $O_2$, $^{12}CO_2$, $^{13}CO_2$) obtained were normalized for a constant sum of all gases and a baseline subtraction was done for $^{12}CO_2$ and $^{13}CO_2$.

### $^{13}CO_2$ labeling experiment of *Populus trichocarpa*

The utility of the new multigas sensing methodology is demonstrated in a labeling experiment that was designed to investigate the allocation of newly assimilated carbon to secondary metabolites. Saplings of *Populus trichocarpa* (see Experimental details) were exposed to $^{13}CO_2$ in the chamber during a two hour pulse labeling experiment (Fig. 2). The Raman gas sensor was connected to the labeling chamber on the opposite side of the $^{13}CO_2$ input to measure the labeled gas after it traveled through the chamber (Fig. 2). The Raman sensor always analyzed the homogenized gas concentration of the labeling chamber. Successive addition of the label was applied to increase the levels of $^{13}C$ that could be incorporated into plant metabolites. Raman gas monitoring was applied to observe the maximum $^{13}CO_2$ concentration and to ensure that the plants took up all the labeled $^{13}C$. The continuous online quantification of the $^{13}CO_2$ level in the chamber allowed for accurate monitoring of the uptake during the labeling period and the precise timing of the second dose of $^{13}CO_2$ (Fig. 3).

First, the labeling chamber was flushed with $CO_2$-free air to decrease the amount of $^{12}CO_2$ from 586 ppm to <100 ppm within 0.5 h. At 0.7 h, $^{13}CO_2$ was chemically generated from $^{13}C$-bicarbonate and diluted hydrochloric acid. A few minutes later the concentration of $^{13}CO_2$ reached its maximum at 298 ppm and then decreased to <100 ppm after 1.6 h due to

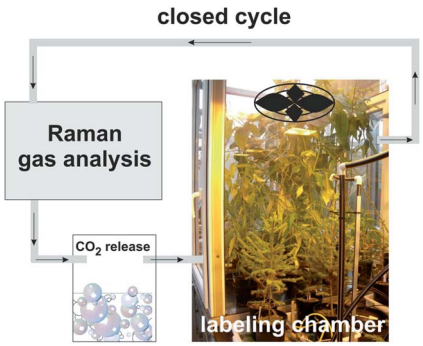


Fig. 2 Schematic setup of the Raman gas analysis of a $^{13}CO_2$ labeling experiment. The Raman gas sensor was connected to the labeling chamber such that the homogenized gas of the chamber was analyzed in a closed cycle. The Raman analysis did not change the gas composition. $^{13}CO_2$ was released chemically and introduced into the chamber by a valve. The inset-photograph of the labeling chamber shows the seedlings of *Populus trichocarpa* under growing lights in order to stimulate photosynthetic uptake of $^{13}CO_2$.

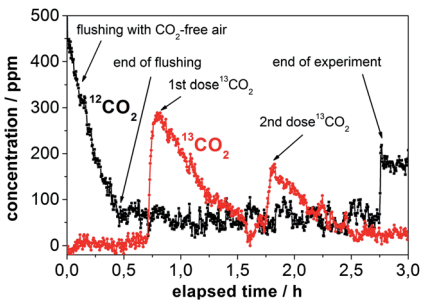


Fig. 3 Online Raman multigas analysis of the $^{13}CO_2$ pulse labeling experiment. The concentrations of $^{12}CO_2$ and $^{13}CO_2$ in the chamber are shown over the duration of the labeling procedure. The relevant steps are assigned: flushing with $CO_2$-free air, release of $^{13}CO_2$, photosynthetic uptake of $^{13}CO_2$ (1st dose and 2nd dose), and opening of the chamber at the end. $^{12}CO_2$, $^{13}CO_2$, and $O_2$ were simultaneously quantified without cross-sensitivity.

photosynthetic uptake by the plants (Fig. 3). After the complete uptake of the first dose, a second dose was administered. The $^{13}CO_2$ concentration reached 182 ppm at 1.8 h and dropped to <100 ppm during the next half hour. At 2.75 h the labeling chamber was opened to ambient air. The concentration of $O_2$ (calculated by a linear fit) rose by approximately 400 ppm during the labeling period, whereas the concentration of $N_2$ did not change significantly.

A major drawback of conventional gas sampling techniques is the extended time needed for data analysis and consequently the small number of data points. In contrast, the high time resolution of Raman gas sensing was exploited for the rapid acquisition of many data points tracking the $^{13}CO_2$-concentration during the course of the labeling, which allowed for kinetic investigations. First-order exponential fitting enabled the very precise determination of time constants (Table 1) and peak concentrations of $^{13}CO_2$ (Table 2).

Two separate labeling runs were performed on different days, and more leaf area and photosynthetically active radiation (PAR) were available inside the labeling chamber in the second run. The comparison of both runs revealed that the amount of $O_2$ produced during the $^{13}CO_2$ labeling period was higher (0.38 mol per day compared to 0.35 mol per day) in run two. Similarly, the uptake of $^{13}CO_2$ over time was faster in the second run, with a decay time of 15.7 min to reduce the amount of $^{13}CO_2$ to $1/e$ of its starting value in comparison to 20.6 min in the first labeling run. All values are summarized in Table 1.

The high time resolution of Raman gas monitoring (Fig. 3) enabled the detection of small deviations from the exponential decay due to fluctuations in natural light intensity, and, by comparison of both doses, it was even possible to confirm that $^{13}CO_2$ uptake by *P. trichocarpa* was faster at higher concentrations of $^{13}CO_2$ within the course of the first dose because the photosynthesis rate of $C_3$ plants is not strictly linear at low concentrations.[15]

An important task in environmental labeling experiments is the correct estimation of the peak concentration of $^{13}CO_2$ in the labeling chamber. Peak concentrations are conventionally calculated based on the mass of the $^{13}C$-bicarbonate used to create the $^{13}CO_2$. However, these approximations overestimate the value in the homogenized chamber atmosphere, due to the immediate photosynthetic $^{13}CO_2$-uptake by the plants in the labeling chamber and the time for the chemical release of $^{13}CO_2$ which broadens the sharpness of the labeling pulse. It is more precise to measure the $^{13}CO_2$-concentration in the labeling chamber online and with rapid data acquisition by means of Raman gas sensing and calculate the peak concentration from the decay equation with high precision by extrapolating back to the time of the dose (Table 2). These peak concentrations of $^{13}CO_2$ were lower with the first addition of $^{13}CO_2$ than those calculated based on the mass of reacted bicarbonate, but the extrapolated values were higher after the second addition of $^{13}CO_2$ in each labeling run (Table 2). This demonstrates that residual $^{13}CO_2$ from the first dose was still present at the addition of the second dose, meaning actual $^{13}CO_2$ values were noticeably higher than expected by standard bicarbonate-weight based calculations (Table 2).

In general, the amount of available data points from the temporally highly resolved Raman spectroscopic gas measurements enabled a very reliable fitting of time dependency curvatures and was well suited for kinetic investigations.

Table 2 Summary of the $^{13}CO_2$ peak concentrations (ppm) released. The calculated values were derived from the weighted $^{13}C$-bicarbonate portion. The extrapolated values were derived from the exponential fit of the measured $^{13}CO_2$ Raman gas curve. Both calculations are in agreement, however the extrapolated Raman gas data deliver more precise information of the homogenized chamber gas atmosphere due to the fast photosynthetic $^{13}CO_2$-uptake during the time of the chemical $^{13}CO_2$-release

| Labeling run | 1st dose calculated [ppm] | 1st dose extrapolated [ppm] | 2nd dose calculated [ppm] | 2nd dose extrapolated [ppm] |
|---|---|---|---|---|
| 1 | 400 | 386 | 200 | 212 |
| 2 | 400 | 381 | 200 | 215 |

## Leaf dark respiration

The labeled plants were further investigated with leaf dark respiration measurements in order to understand $^{13}CO_2$ exchange over time. Approximately 24 h after the $^{13}C$-labeling, *P. trichocarpa* leaves of a known area were enclosed in a dark chamber, and the concentrations of $O_2$, $^{12}CO_2$, and $^{13}CO_2$ were continuously recorded. The fluxes of all gases were calculated based on changes of the gas concentrations over time in the enclosed headspace. The fluxes were related to a leaf area that was based on one side of the leaf only to represent the area where the stomata are located. The respired gases were circulated through the instrument and returned to the chamber without consumption or alteration by the measurement. Ambient air was measured after one hour to validate the stability of experimental setting. A linear fit of the gas concentrations over time yielded rates for the uptake of $O_2$ and $CO_2$ production (Fig. 4). The current detection limit of the device for

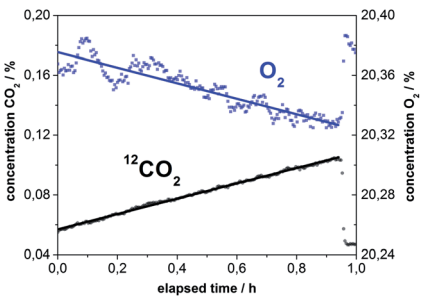


Fig. 4 Quantification of $O_2$ and $CO_2$ during the course of a leaf dark respiration measurement of *Populus trichocarpa*. The amount of $O_2$ decreased and the concentration of $CO_2$ increased linearly with respect to time. The slopes of the linear fits yield the respiration rates for both gases with just a single measurement. Ambient air was measured as a reference at the end of the experiment, and the concentrations of $O_2$ and $CO_2$ leap back to the correct starting values of air.

$^{12}CO_2$ was 48 ppm ($\sigma = 3$) which results in a limit of detectable exchange rate of 0.12 μmol $m^{-2}$ $h^{-1}$. The additional $^{13}CO_2$ efflux rate added by the highly diluted label from the plant was below this level. The leaf dark respiration measurements resulted in an $O_2$ consumption rate of 1.81 μmol $m^{-2}$ $h^{-1}$ and a $CO_2$ production rate of 1.80 μmol $m^{-2}$ $h^{-1}$ for immature leaves. In comparison, mature leaves consumed only 0.70 μmol $m^{-2}$ $h^{-1}$ of $O_2$ and produced just 0.74 μmol $m^{-2}$ $h^{-1}$ of $CO_2$. These results indicate that the respiration rates of immature leaves are more than twice as high as the respiration rates of mature leaves. Distinctly higher dark respiration rates of immature leaves are also reported in the literature.[16] Simultaneous Raman spectroscopic quantification of $O_2$ and $CO_2$ also allowed for the calculation of the respiratory quotient (RQ) which yields information about the compounds being metabolized and respired. Deviations in the respiratory quotient arise from differing carbon–oxygen ratios of substrates or the formation of byproducts.[17] The RQ values were ~1 for all leaves, indicating the combustion of starch.[18]

## Conclusions and outlook

This work demonstrates the unique capabilities of innovative cavity enhanced Raman gas monitoring for the control and analysis of $^{13}CO_2$-labeling experiments. Enhanced Raman gas sensing is superior to conventional Raman gas spectroscopy, due to the strong power build up to 100 W within the cavity (while maintaining low instrument power consumption) and outperforms other gas sensing techniques for the rapid and simultaneous analysis of multiple gases in a labeling chamber while eliminating sample collections and delayed analyses. The technique is non-consumptive, such that the measurements can be performed in a closed cycle with the labeling chamber without altering the gas composition. The high time resolution of the Raman measurement enables the acquisition of a huge number of data points, which tremendously increases the accuracy of kinetic investigations. Thus, it was possible to determine precise uptake rates and peak concentrations of $^{13}CO_2$ in the pulse labeling of *P. trichocarpa*. Additionally, the simultaneous measurements of $CO_2$ and $O_2$ allowed for calculation of photosynthetic rates for both gases at once which correlated with the leaf area as well as the photosynthetically active radiation inside the labeling chamber. The investigation of leaf dark respiration of *P. trichocarpa* revealed that the respiration rate of immature leaves was more than twice as high compared to mature leaves. Simultaneous Raman gas quantification of $O_2$ and $CO_2$ enabled the calculation of the respiratory quotient, which is an indicator of the chemistry of metabolites that are fueling respiration, or can indicate the net effects of gas transport *via* the plant transpiration stream. Monitoring of $^{13}CO_2$, $^{12}CO_2$, and $O_2$ also allows for quantification of the amount of label that got fixed by the plant and the $^{13}C : {}^{12}C$-ratio.

Cavity enhanced Raman multigas sensing was shown to be a very versatile new technique for monitoring the amount of label incorporation in $^{13}CO_2$-labeling experiments and it is also capable of rapidly analyzing the respiration quotient, an ecophysiologically important parameter. This new technique is affordable and very robust due to the linearity of signal intensity to analyte concentration. We therefore anticipate that cavity enhanced Raman spectroscopy (CERS) will become an important tool for labeling experiments in environmental research.

## Acknowledgements

Funding of the research project by the Collaborative Research Centre 1076 "AquaDiva" from the Deutsche Forschungsgemeinschaft (DFG) is gratefully acknowledged. The authors thank Dr. Willi Brand (MPI-BGC) for the calibration gases.

## References

1 M. S. Carbone and S. E. Trumbore, Contribution of new photosynthetic assimilates to respiration by perennial grasses and shrubs: residence times and allocation patterns, *New Phytol.*, 2007, **176**(1), 124–135.
2 P. Högberg, M. N. Högberg, S. G. Göttlicher, N. R. Betson, S. G. Keel, D. B. Metcalfe, C. Campbell, A. Schindlbacher, V. Hurry, T. Lundmark, S. Linder and T. Näsholm, High temporal resolution tracing of photosynthate carbon from the tree canopy to forest soil microorganisms, *New Phytol.*, 2008, **177**(1), 220–228.
3 T. Arnold and J. Schultz, Induced sink strength as a prerequisite for induced tannin biosynthesis in developing leaves of *Populus*, *Oecologia*, 2002, **130**(4), 585–593.
4 E. C. Connor, A. S. Rott, M. Zeder, F. Juttner and S. Dorn, 13C-labelling patterns of green leaf volatiles indicating different dynamics of precursors in *Brassica* leaves, *Phytochemistry*, 2008, **69**(6), 1304–1312.
5 D. Yakir and L. d. S. L. Sternberg, The use of stable isotopes to study ecosystem gas exchange, *Oecologia*, 2000, **123**(3), 297–311.
6 D. A. Herms and W. J. Mattson, The Dilemma of Plants: To Grow or Defend, *Q. Rev. Biol.*, 1992, **67**(3), 283.
7 D. Epron, M. Bahn, D. Derrien, F. A. Lattanzi, J. Pumpanen, A. Gessler, P. Hogberg, P. Maillard, M. Dannoura, D. Gerant and N. Buchmann, Pulse-labelling trees to study carbon allocation dynamics: a review of methods, current knowledge and future prospects, *Tree Physiol.*, 2012, **32**(6), 776–798.
8 (*a*) A. Saveyn, K. Steppe, M. A. McGuire, R. Lemeur and R. O. Teskey, Stem respiration and carbon dioxide efflux of young *Populus deltoides* trees in relation to temperature and xylem carbon dioxide concentration, *Oecologia*, 2008, **154**(4), 637–649; (*b*) S. Hunt, Measurements of photosynthesis and respiration in plants, *Physiol. Plant.*, 2003, **117**(3), 314–325.
9 (*a*) T. Frosch, S. Koncarevic, K. Becker and J. Popp, Morphology-sensitive Raman modes of the malaria pigment hemozoin, *Analyst*, 2009, **134**(6), 1126–1132; (*b*) T. Frosch and J. Popp, Structural analysis of the antimalarial drug halofantrine by means of Raman spectroscopy and density functional theory calculations, *J. Biomed. Opt.*, 2010, **15**(4),

041516; (*c*) T. Frosch, M. Schmitt, G. Bringmann, W. Kiefer and J. Popp, Structural analysis of the anti-malaria active agent chloroquine under physiological conditions, *J. Phys. Chem. B*, 2007, **111**(7), 1815–1822; (*d*) T. Frosch, M. Schmitt, K. Schenzel, J. H. Faber, G. Bringmann, W. Kiefer and J. Popp, *In vivo* localization and identification of the antiplasmodial alkaloid dioncophylline A in the tropical liana *Triphyophyllum peltatum* by a combination of fluorescence, near infrared Fourier transform Raman microscopy, and density functional theory calcula, *Biopolymers*, 2006, **82**(4), 295–300.

10 (*a*) T. Frosch, T. Meyer, M. Schmitt and J. Popp, Device for Raman difference spectroscopy, *Anal. Chem.*, 2007, **79**(16), 6159–6166; (*b*) T. Frosch, M. Schmitt, T. Noll, G. Bringmann, K. Schenzel and J. Popp, Ultrasensitive *in situ* tracing of the alkaloid dioncophylline A in the tropical liana *Triphyophyllum peltatum* by applying deep-UV resonance Raman microscopy, *Anal. Chem.*, 2007, **79**(3), 986–993; (*c*) T. Frosch, N. Tarcea, M. Schmitt, H. Thiele, F. Langenhorst and J. Popp, UV Raman Imaging - A Promising Tool for Astrobiology: Comparative Raman Studies with Different Excitation Wavelengths on SNC Martian Meteorites, *Anal. Chem.*, 2007, **79**(3), 1101–1108; (*d*) T. Frosch, D. Yan and J. Popp, Ultrasensitive Fiber Enhanced UV Resonance Raman Sensing of Drugs, *Anal. Chem.*, 2013, **85**(13), 6264–6271.

11 (*a*) T. Frosch, S. Koncarevic, L. Zedler, M. Schmitt, K. Schenzel, K. Becker and J. Popp, In situ localization and structural analysis of the malaria pigment hemozoin, *J. Phys. Chem. B*, 2007, **111**(37), 11047–11056; (*b*) T. Frosch, B. Küstner, S. Schlücker, a. Szeghalmi, M. Schmitt, W. Kiefer and J. Popp, In vitro polarization-resolved resonance Raman studies of the interaction of hematin with the antimalarial drug chloroquine, *J. Raman Spectrosc.*, 2004, **35**(10), 819–821; (*c*) T. Frosch and J. Popp, Relationship between molecular structure and Raman spectra of quinolines, *J. Mol. Struct.*, 2009, **924–926**, 301–308; (*d*) T. Frosch, M. Schmitt and J. Popp, In situ UV resonance Raman micro-spectroscopic localization of the antimalarial quinine in cinchona bark, *J. Phys. Chem. B*, 2007, **111**(16), 4171–4177; (*e*) T. Frosch, M. Schmitt and J. Popp, Raman spectroscopic investigation of the antimalarial agent mefloquine, *Anal. Bioanal. Chem.*, 2007, **387**(5), 1749–1757.

12 (*a*) T. Frosch, R. Keiner, B. Michalzik, B. Fischer and J. Popp, Investigation of gas exchange processes in peat bog ecosystems by means of innovative Raman gas spectroscopy, *Anal. Chem.*, 2013, **85**(3), 1295–1299; (*b*) R. Keiner, T. Frosch, S. Hanf, A. Rusznyak, D. M. Akob, K. Kusel and J. Popp, Raman Spectroscopy-An Innovative and Versatile Tool To Follow the Respirational Activity and Carbonate Biomineralization of Important Cave Bacteria, *Anal. Chem.*, 2013; (*c*) R. Salter, J. Chu and M. Hippler, Cavity-enhanced Raman spectroscopy with optical feedback cw diode lasers for gas phase analysis and spectroscopy, *Analyst*, 2012, **137**(20), 4669–4676.

13 D. A. King and R. J. Pittaro, Simple diode pumping of a power-build up cavity, *Opt. Lett.*, 1998, **23**(10), 774–776.

14 H. Howardlock and B. Stoicheff, Raman intensity measurements of the Fermi diad $\nu_1$, $2\nu_2$ in $^{12}CO_2$ and $^{13}CO_2$, *J. Mol. Spectrosc.*, 1971, **37**(2), 321–326.

15 T. D. Sharkey, Photosynthesis in intact leaves of C3 plants: Physics, physiology and rate limitations, *Bot. Rev.*, 1985, **51**(1), 53–105.

16 D. I. Dickmann, Photosynthesis and Respiration by Developing Leaves of Cottonwood (*Populus deltoides* Bartr.), *Bot. Gaz.*, 1971, **132**(4), 253–259.

17 J. Azcon-Bieto, H. Lambers and D. A. Day, Effect of Photosynthesis and Carbohydrate Status on Respiratory Rates and the Involvement of the Alternative Pathway in Leaf Respiration, *Plant Physiol.*, 1983, **72**(3), 598–603.

18 N. G. McDowell, Mechanisms linking drought, hydraulics, carbon metabolism, and vegetation mortality, *Plant Physiol.*, 2011, **155**(3), 1051–1059.

 